Received: 10 April 2019 | Revised: 17 September 2019 | Accepted: 14 October 2019

DOI: 10.1002/bit.27202

BIOTECHNOLOGY BIOENGINEERING WILEY

ARTICLE

Xylose assimilation enhances the production of isobutanol in engineered *Saccharomyces cerevisiae*

Stephan Lane[1,2,3] | Yanfei Zhang[4] | Eun Ju Yun[1] | Leah Ziolkowski[1,2,3] | Guochang Zhang[1] | Yong-Su Jin[1,2,3] | José L. Avalos[4,5,6]

[1]Carl R. Woese Institute for Genomic Biology, University of Illinois at Urbana-Champaign, Urbana, Illinois

[2]DOE Center for Advanced Bioenergy and Bioproducts Innovation, University of Illinois at Urbana-Champaign, Urbana, Illinois

[3]Department of Food Science and Human Nutrition, University of Illinois at Urbana-Champaign, Urbana, Illinois

[4]Department of Chemical and Biological Engineering, Princeton University, Princeton, New Jersey

[5]Andlinger Center for Energy and the Environment, Princeton University, Princeton, New Jersey

[6]Department of Molecular Biology, Princeton University, Princeton, New Jersey

Correspondence
Yong-Su Jin, Carl R. Woese Institute for Genomic Biology, University of Illinois at Urbana-Champaign, Urbana, IL.
Email: ysjin@illinois.edu

José L. Avalos, Department of Chemical and Biological Engineering, Princeton University, Princeton, NJ.
Email: javalos@princeton.edu

Funding information
DOE Center for Advanced Bioenergy and Bioproducts Innovation, Grant/Award Numbers: DE-SC0018420, DE-SC0019363

Abstract

Bioconversion of xylose—the second most abundant sugar in nature—into high-value fuels and chemicals by engineered *Saccharomyces cerevisiae* has been a long-term goal of the metabolic engineering community. Although most efforts have heavily focused on the production of ethanol by engineered *S. cerevisiae*, yields and productivities of ethanol produced from xylose have remained inferior as compared with ethanol produced from glucose. However, this entrenched focus on ethanol has concealed the fact that many aspects of xylose metabolism favor the production of nonethanol products. Through reduced overall metabolic flux, a more respiratory nature of consumption, and evading glucose signaling pathways, the bioconversion of xylose can be more amenable to redirecting flux away from ethanol towards the desired target product. In this report, we show that coupling xylose consumption via the oxidoreductive pathway with a mitochondrially-targeted isobutanol biosynthesis pathway leads to enhanced product yields and titers as compared to cultures utilizing glucose or galactose as a carbon source. Through the optimization of culture conditions, we achieve 2.6 g/L of isobutanol in the fed-batch flask and bioreactor fermentations. These results suggest that there may be synergistic benefits of coupling xylose assimilation with the production of nonethanol value-added products.

KEYWORDS
branched-chain alcohols, isobutanol, metabolic engineering, *Saccharomyces cerevisiae*, xylose

1 | INTRODUCTION

Over the past few decades, significant research has focused on the production of biofuels from renewable biomass (Bilal, Iqbal, Hu, Wang, & Zhang, 2018). Current commercial biofuel production focuses mainly on the bioconversion of hexose sugars, such as those in corn starch and sugarcane, into ethanol (Bordonal et al., 2018; Marques, Moreno, Ballesteros, & Gírio, 2017). However, these feedstocks also participate in the food supply and therefore ignite the food versus fuel debate: Heavy utilization of human-edible biomass may potentially increase food prices and exacerbate food insecurity (Filip, Janda, Kristoufek, & Zilbermam, 2017). To bypass this debate, the bioconversion of lignocellulosic biomass has been proposed. In contrast to the human-edible sugars used as feedstocks in first-generation bioethanol, lignocellulosic biomass does not participate in the food supply and is comprised of cellulose, hemicellulose, and lignin, which can be depolymerized into a mixture of hexose and pentose sugars (Lane, Dong, & Jin, 2018). In addition to avoiding the food versus fuel debate, lignocellulosic feedstocks are

desirable due to their presence as agricultural wastes, overall high abundance, and relatively low cost (Ho, Ngo, & Guo, 2014).

Among microbes suitable for use in lignocellulosic bioconversion processes, the yeast *Saccharomyces cerevisiae* has been highly preferred due to its exceptional ethanol tolerance, relatively high resistance to fermentation inhibitors, and ease of engineering (Kwak & Jin, 2017). However, *S. cerevisiae* cannot natively assimilate xylose and thus significant efforts have been put towards engineering xylose-consuming yeast strains (Kim, Park, Jin, & Seo, 2013). Primarily, two xylose metabolism pathways have been employed: the isomerase pathway consisting of xylose isomerase and xylulose kinase (XK), and the oxidoreductive pathway consisting of xylose reductase, xylitol dehydrogenase, and XK (Kwak & Jin, 2017; Moysés, Reis, de Almeida, de Moraes, & Torres, 2016).

In most cases, research involving engineered xylose-consuming yeasts has focused on the production of ethanol. However, accumulating evidence shows that utilizing xylose as a carbon source may allow enhanced production of a variety of nonethanol products (Lane et al., 2018). Because xylose does not elicit the Crabtree effect in *S. cerevisiae*, metabolic fluxes during xylose fermentation by engineered *S. cerevisiae* are not rigidly directed towards ethanol, and maybe more amenable to redirection towards an alternative target product (Kildegaard, Wang, Chen, Nielsen, & Borodina, 2015).

In this study, we aimed to produce the advanced biofuel isobutanol from xylose using engineered yeast. The isobutanol biosynthesis pathway employed in this study consists of the endogenous acetolactate synthase (*ILV2*), ketol-acid reductoisomerase (*ILV5*), and dihydroxyacid dehydratase (*ILV3*) coupled with the *Lactococcus lactis* α-ketoisovalerate decarboxylase (*Kivd*), and alchohol dehydrogenase ($AdhA^{RE1}$) which has been engineered for increased affinity to isobutyraldehyde (Figure 1; Bastian et al., 2011). These biosynthetic enzymes are targeted to the mitochondria when expressed in yeast, which increases the production of isobutanol (Avalos, Fink, & Stephanopoulos, 2013). Although this initial report of compartmentalizing the isobutanol pathway in the mitochondria for enhanced isobutanol production used glucose as a carbon source, glucose is known to lead to reduced mitochondrial genesis (Egner, Jakobs, & Hell, 2002). We, therefore, aimed to compare the effects of different carbon sources—specifically glucose, galactose, and xylose—on the production of isobutanol in an engineered yeast containing a mitochondrial-compartmentalized isobutanol production pathway.

2 | MATERIALS AND METHODS

2.1 | Strains and plasmids

This study used the xylose-consuming SR8 strain (Kim, Skerker et al., 2013), which expresses the oxidoreductive xylose assimilation pathway (*XYL1*, *XYL2*, and *XYL3*) and contains a mutation in the *PHO13* (Xu et al., 2016) gene and a deletion of *ALD6*. The auxotrophic SR8 *ura*$^-$ strain was created as described previously (G. C. Zhang et al., 2014) by deleting the *URA3* gene using CRISPR genome editing. The mitochondrial-localized isobutanol pathway was expressed by transformation with the plasmid pJA180 (Avalos et al., 2013), and plasmid pRS426 (Christianson, Sikorski, Dante, Shero, & Hieter, 1992) was used as empty vector control.

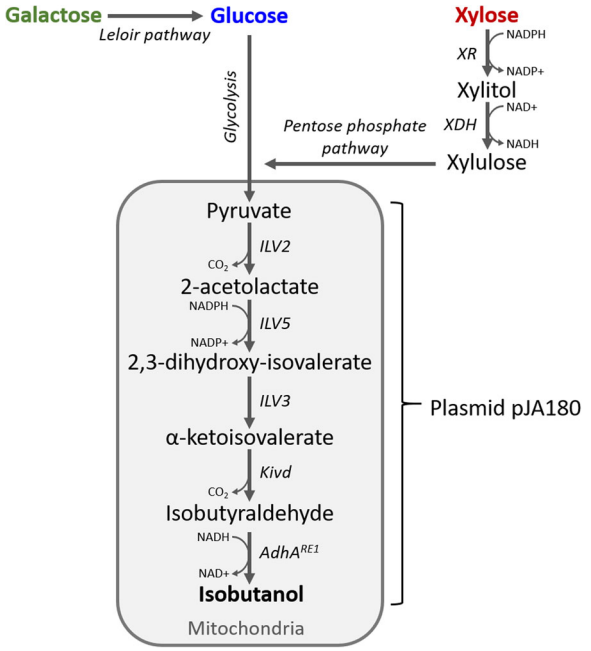

FIGURE 1 Metabolic pathways for bioconversion of xylose to isobutanol. Xylose reductase (*XR*) converts xylose to xylitol, which is then converted to xylulose by xylitol dehydrogenase (*XDH*). Xylulose is then phosphorylated by xylulose kinase where it enters the pentose phosphate pathway and central carbon metabolism. Plasmid pJA180, the isobutanol production plasmid used in this study, overexpresses endogenous *ILV2*, *ILV3*, and *ILV5* with mitochondrial-targeted *Lactococcus lactis Kivd* and engineered $AdhA^{RE1}$ [Color figure can be viewed at wileyonlinelibrary.com]

2.2 | Media and culture conditions

This study employed a nutrient-rich Verduyn (NRV) medium described previously with some modifications (van Hoek, De Hulster, Van Dijken, & Pronk, 2000), which contained 15 g/L $(NH_4)_2SO_4$, 8 g/L KH_2PO_4, 3 g/L $MgSO_4$, with 10 ml/L trace element solution and 12 ml/L vitamin solution. The trace element solution was autoclaved for sterilization and contained 15 g/L ethylenediaminetetraacetic acid, 5.75 g/L $ZnSO_4$, 0.32 g/L $MnCl_2$, 0.5 g/L $CuSO_4$, 0.47 g/L $CoCl_2$, 0.48 g/L Na_2MoO_4, 2.9 g/L $CaCl_2$, and 2.8 g/L $FeSO_4$. The vitamin solution was filter sterilized and contained 0.05 g/L biotin, 1 g/L calcium pantothenate, 1 g/L nicotinic acid, 25 g/L myo-inositol, 1 g/L thiamine hydrochloride, 1 g/L pyridoxol hydrochloride, and 0.2 g/L *p*-aminobenzoic acid. $CaCO_3$ (20 g/L) was supplemented to flasks to maintain pH near 6. Feed solution for fed-batch experiments contained 9 g/L KH_2PO_4, 2.5 g/L $MgSO_4$, 3.5 g/L K_2SO_4, 0.28 g/L Na_2SO_4, 400 g/L xylose, 10 ml/L trace element solution, and 12 ml/L vitamin solution.

Preculture was performed for 24 hr in culture tubes with 4 ml NRV medium with 20 g/L glucose. Flask fermentations were performed with 25 ml NRV media in 125 ml flasks at 30°C. Unless

otherwise specified, flasks were agitated at 100 rotations per minute (rpm) and initial cell concentrations were set to an optical density 600 (OD_{600}) of 0.03.

The bioreactor experiment was initiated with a cell density equal to an OD_{600} of 0.03 in an initial volume of 1 L NRV medium and 20 g/L xylose. After consumption of the initial xylose, a single pulse feeding was used to increase xylose to 80 g/L. Agitation was set to 200 rpm, airflow was set to 0.5 L/min, and pH was maintained at 5.8 using 5 M NaOH.

2.3 | Analytical methods

Biomass was quantified as the absorbance at 600 nm (OD_{600}) using a Biomate 5 ultraviolet–visible spectrophotometer (Thermo Fisher Scientific, NY). The concentration of sugars, glycerol, xylitol, and ethanol was measured using high-performance liquid chromatography (Agilent, Santa Clara, CA) with a Rezex ROA-Organic Acid H^+ (8%) column (Phenomenex Inc.,) while the concentration of isobutanol was determined using gas chromatography (GC; Agilent Technologies 7890A) with a flame ionization detector (FID) equipped with an HP-INNOWax column. The GC oven temperature was initially held at 30°C for 3 min and was then increased at a rate of 35°C/min to 225°C then held for 2 min. The injector temperature was held at 225°C, and the FID detector was held at 330°C. An injection volume of 1 μl and a split ratio of 2:1 was used for the analysis. Helium was used as a carrier gas.

2.4 | Metabolite profiling

Metabolites were extracted using the fast filtration method (S. Kim et al., 2013) and profiled as described previously (Yun et al., 2018). Biological duplicates were used along with technical triplicates for a total of six analyzed samples per culture condition. SR8-Iso was grown to mid-exponential phase in NRV medium with glucose or xylose as a carbon source. One milliliter of culture was then filtered through a 0.45 μm nylon membrane filter (Whatman, Piscataway, NJ) followed by washing with 2 ml of distilled water. The filter and filtered cells were then together submerged into a microfuge tube containing 200 μl of acid-washed 425–600 μm glass beads and 1 ml of a cold 1:1 volume mixture of acetonitrile and water. Metabolites were then extracted by vortexing for 3 min followed by pelleting of cell debris by centrifuging at 15,000 rpm at 4°C for 5 min. The supernatant was then collected and dried in a speed vacuum drier.

Derivatization of metabolites was performed by methoxyamination and silylation. First, 5 μl of 40 mg/ml methoxyamine hydrochloride in pyridine (Sigma-Aldrich, St. Louis, MO) was added to the dried metabolites followed by incubation for 90 min at 30°C. Next, 45 μl of *N*-methyl-*N*-trimethylsilyltrifluoroacetamide (Sigma-Aldrich, St. Louis, MO) was added followed by incubation for 30 min at 37°C.

Derivatized samples were next analyzed through GC—mass spectrometry (MS) following the protocol described previously (Yun et al., 2018). Briefly, the derivatized samples were analyzed in an Agilent 7890A GC/5975C MSD system (Agilent Technologies) equipped with an RTX-5Sil MS capillary column (30 m × 0.25 mm, 0.25 μm film thickness; Restek, Bellefonte, PA) and an integrated guard column. A 1 μl sample was injected into the GC inlet in splitless mode. The oven temperature was set to the following: 150°C for 1 min, then increased to 330°C at 20°C/min, and held at 330°C for 5 min. The mass spectra were recorded in a scan range 85–500 m/z at an electron impact of 70 eV. The temperature of the ion source was 230°C while the transfer line was 280°C.

The raw data obtained from GC/MS analysis were preprocessed in automated mass spectral deconvolution and identification system software (Stein, 1999) for peak detection and deconvolution of mass spectra, which was then analyzed by SpectConnect (http://spectconnect.mit.edu; Styczynski et al., 2007) for peak alignment and generation of the data matrix using the Golm Metabolome Database mass spectral reference library (Kopka et al., 2005). The normalized abundance values for each metabolite were calculated by dividing peak intensity by the dry cell weight. Statistica (version 7.1; StatSoft, Palo Alto, CA) and MultiExperiment Viewer software (Ochs, Casagrande, & Davuluri, 2010) were used for statistical analysis and generation of heat maps, respectively.

3 | RESULTS

3.1 | Comparison of isobutanol production from glucose, galactose, and xylose

Strain SR8-Iso was created by transforming SR8 *ura*$^-$ with plasmid pJA180, containing the genes of mitochondrial isobutanol biosynthetic pathway: *S. cerevisiae ILV2*, *ILV3*, and *ILV5* with *L. lactis Kivd* and engineered *AdhA*^{RE1} (Figure 1); the last two genes targeted to mitochondria using the *COXIV* mitochondrial localization signal (Avalos et al., 2013). As a control, empty vector pRS426 (Mumberg, Müller, & Funk, 1995) was also transformed into SR8 *ura*$^-$ yielding SR8-C. These strains were then cultured with approximately 40 g/L of either glucose (Figure S1), galactose (Figure S2), or xylose (Figure S3) as a sole carbon source. The SR8-Iso strain ferments each sugar more slowly and, apart from the glucose culture, yields less ethanol than the control strain SR8-C. As expected, the SR8-Iso strain consistently produces more isobutanol than the empty vector control strain SR8-C.

The SR8-Iso strain grows, consumes sugar, and produces ethanol more slowly on xylose than any other carbon source (Figure 2a). However, culturing the SR8-Iso strain on xylose yields nearly sixfold more isobutanol (24.6 ± 0.04 mg isobutanol/g xylose) than any other carbon source (4.2 ± 0.06 mg isobutanol/g glucose and 4.3 ± 0.02 mg isobutanol/g galactose; Figure 2b). Starting with about 40 g/L of sugar, 872 ± 6.8 mg/L of isobutanol is produced from xylose while 156 ± 2.1 mg/L and 168 ± 0.8 mg/L of isobutanol are produced from glucose and galactose, respectively. In contrast, the SR8-Iso strain produces the most ethanol from glucose (12.8 ± 0.1 g/L ethanol at a yield of 0.34 g ethanol/g sugar) followed by galactose (11.2 ± 0.07 g/L ethanol at a yield of 0.28 g ethanol/g sugar), while the least amount of ethanol is produced from xylose (6.2 ± 0.01 g/L ethanol at a yield of 0.18 g ethanol/g sugar).

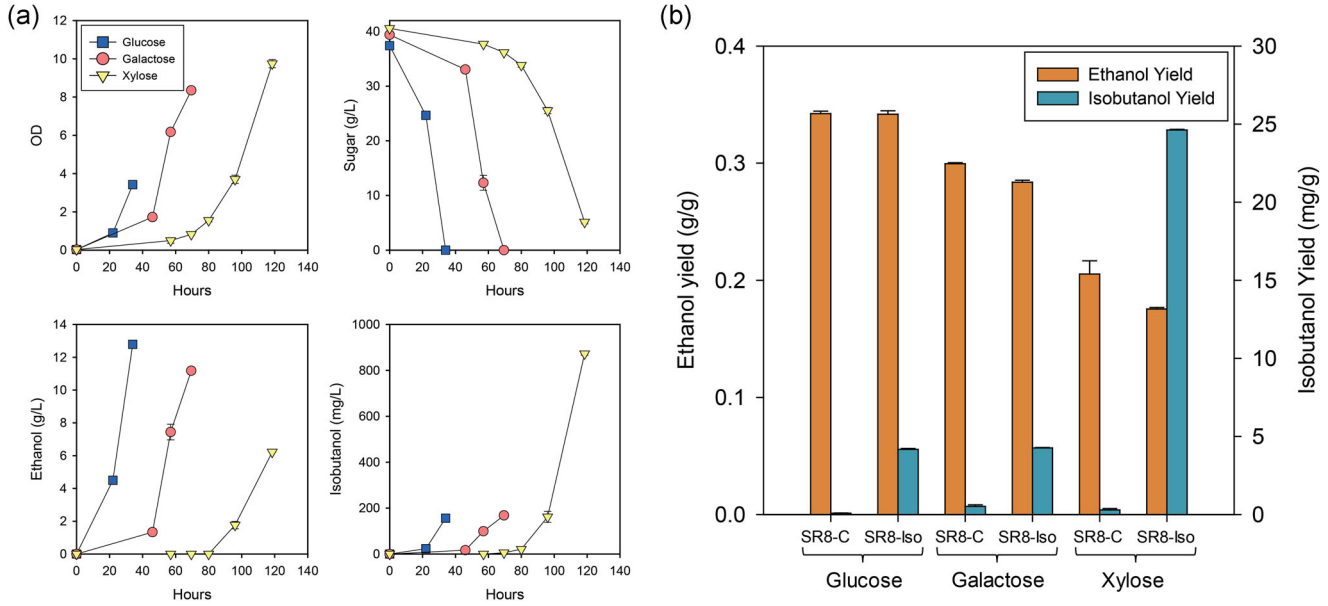

FIGURE 2 Carbon source affects the production of isobutanol. (a) Fermentation profiles of SR8-Iso cultured on glucose (blue squares), galactose (pink circles), or xylose (yellow triangles) displaying cell density (top left), sugar (top right), ethanol (bottom left), and isobutanol (bottom right) concentrations. Fermentations were performed in 125 ml flasks containing 25 ml medium and 20 g/L $CaCO_3$ at 30°C and 100 rpm with an initial cell inoculum equal to an OD_{600} of 0.03. Data points are the average of two biological duplicates. Error bars indicate standard deviations and are not visible when smaller than the symbol size. (b) Ethanol and isobutanol yield the SR8-Iso and control SR8-C strains cultured on glucose, galactose, and xylose under the same conditions. Displayed values are the average of two biological duplicates with error bars indicating standard deviations. OD, optical density; rpm, rotations per minute [Color figure can be viewed at wileyonlinelibrary.com]

3.2 | Optimizing bioconversion of xylose to isobutanol by manipulating fermentation parameters

We next aimed to optimize the production of isobutanol from xylose by varying the fermentation parameters of initial sugar concentration, agitation, and initial cell inoculum. Although the initial xylose concentration largely impacts the production of ethanol, there are no large changes in the yield of isobutanol (Figure 3a). However, culturing with lower initial xylose (20 g/L) leads to faster cell growth, sugar consumption, and isobutanol production than higher amounts of xylose (40 or 80 g/L) (Figure S4). In contrast, the rate of agitation substantially impacts the production of both ethanol and isobutanol (Figures 3b and S5). While ethanol production increases as agitation are reduced, isobutanol is most optimally produced from xylose with flask agitation at 100 rpm. Similarly, initial cell inoculum has a large impact on the production of isobutanol (Figures 3c and S6). By culturing with an initial cell inoculum equal to an OD_{600} of 0.003, the isobutanol yield from xylose is 36.1 ± 1.2 mg isobutanol/g xylose, compared with 27.1 ± 1.1 mg isobutanol/g xylose, and 23.7 ± 0.4 mg isobutanol/g xylose for initial cell inoculums of OD_{600} equal to 0.03

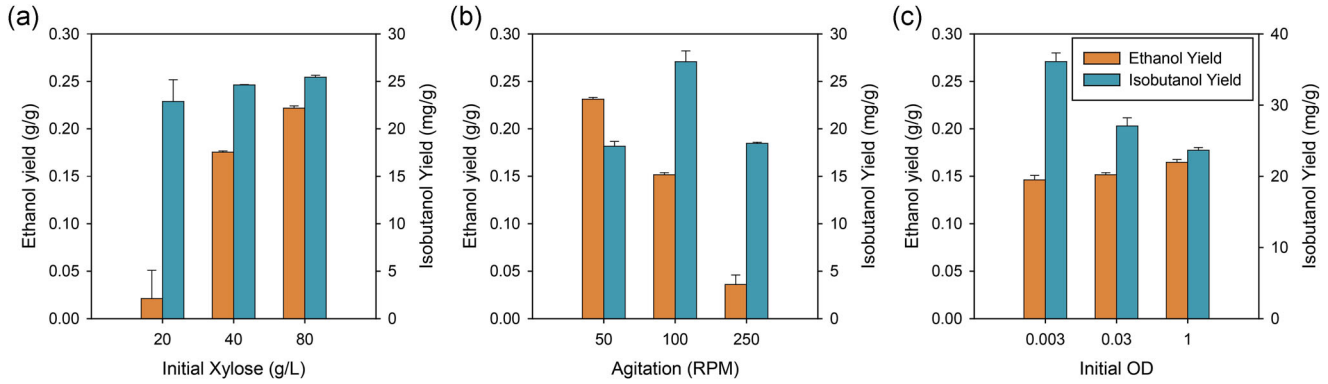

FIGURE 3 Optimization of isobutanol production in strain SR8-Iso. The effects of (a) initial sugar concentration, (b) agitation, and (c) initial cell inoculum on ethanol (orange bars) and isobutanol (blue bars) yields. Displayed values are the average of two biological duplicates with error bars indicating standard deviations. Yields are calculated from fermentations performed in 125 ml flasks containing 25 ml medium and 20 g/L $CaCO_3$ at 30°C. Figure 2a,b was performed with initial cell inoculum equal to an OD_{600} of 0.03, Figure 2a,c were performed at 100 rpm, and Figure 2b,c were performed with an initial xylose concentration of 40 g/L. Full fermentation profiles for Figure 2a,b, and c can be found in Figures S4, S5, and S6, respectively. OD, optical density; rpm, rotations per minute [Color figure can be viewed at wileyonlinelibrary.com]

and 1, respectively. However, lower inoculums result in significantly longer fermentation times; 160 hr is required to consume 40 g/L of xylose when initial OD_{600} = 0.003 as compared with 66 hr for initial OD_{600} = 1.

Using this information, we performed a fed-batch fermentation aiming to produce a high titer of isobutanol. We began with 20 g/L xylose to maximize production rates and, to strike a balance between high yields and a reasonable fermentation length, we inoculated the fermentation with an initial OD_{600} equal to 0.1. Once available xylose reached near or below 10 g/L, additional xylose was fed to replenish the medium to near 20 g/L xylose. The first xylose feeding occurred around 100 hr after the initialization of the fermentation. In total, nine separate feedings occurred throughout the fermentation in addition to the initial 20 g/L xylose provided at the start of the fermentation. In addition, the yield of isobutanol decreases throughout the fermentation. The first 40 g/L of consumed xylose leads to production of around 1 g/L isobutanol, but the final 40 g/L of consumed xylose increases the isobutanol titer by only about 0.4 g/L (Figure 4). In total, 2.56 g/L isobutanol is produced from roughly 190 g/L consumed xylose.

Next, we performed a 1 L bioreactor fermentation to investigate the potential for scaling up. Although we attempted to emulate our strategy during flask fed-batch fermentation of starting with 20 g/L xylose followed by repeated feeding to 20 g/L xylose, this method does not lead to substantial production of isobutanol (data not shown). Instead, starting with 20 g/L of xylose, allowing consumption to <5 g/L of xylose, then feeding to 80 g/L of xylose leads to the production of 2.6 g/L of isobutanol in a bioreactor (Figure 5).

3.3 | Metabolite profiling of isobutanol-producing yeast during xylose and glucose fermentation

To gain some insight into why xylose assimilation leads to a nearly sixfold improvement in the production of isobutanol as compared to glucose fermentation, we next performed metabolite profiling to obtain a systems-level analysis of the strains cultured in different carbon sources (Figure 6). We thus cultured the SR8-Iso strain in NRV medium with 40 g/L of either glucose or xylose as carbon sources and sampled for metabolite analysis in the mid-exponential phase. Metabolites were extracted, derivatized, and profiled as described in the materials and methods. Principle component analysis shows a clear separation between the metabolite profiles obtained from glucose and xylose cultures (Figure S7). Notably, culturing on xylose led to an increased accumulation of valine, a key metabolite related to the isobutanol production pathway.

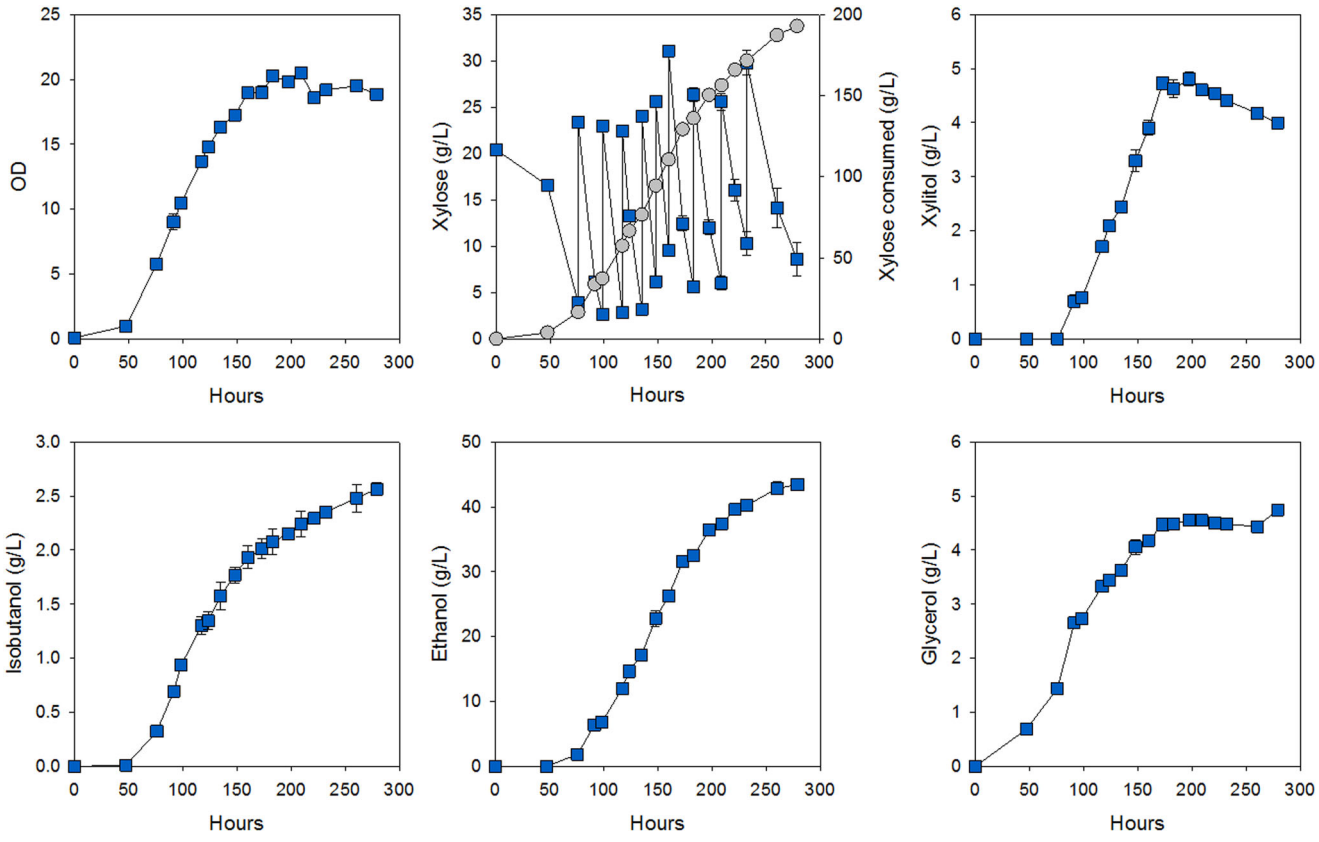

FIGURE 4 Fed-batch fermentation for isobutanol production. Fed-batch fermentation performed in 125 ml flask containing 25 ml medium and 20 g/L $CaCO_3$ at 30°C and 100 rpm with an initial cell inoculum equal to an OD_{600} of 0.1. Concentrations are shown as blue squares while the total consumed xylose is shown as a gray circle. Data points are the average of two biological duplicates. Error bars indicate standard deviations and are not visible when smaller than the symbol size. OD, optical density; rpm, rotations per minute [Color figure can be viewed at wileyonlinelibrary.com]

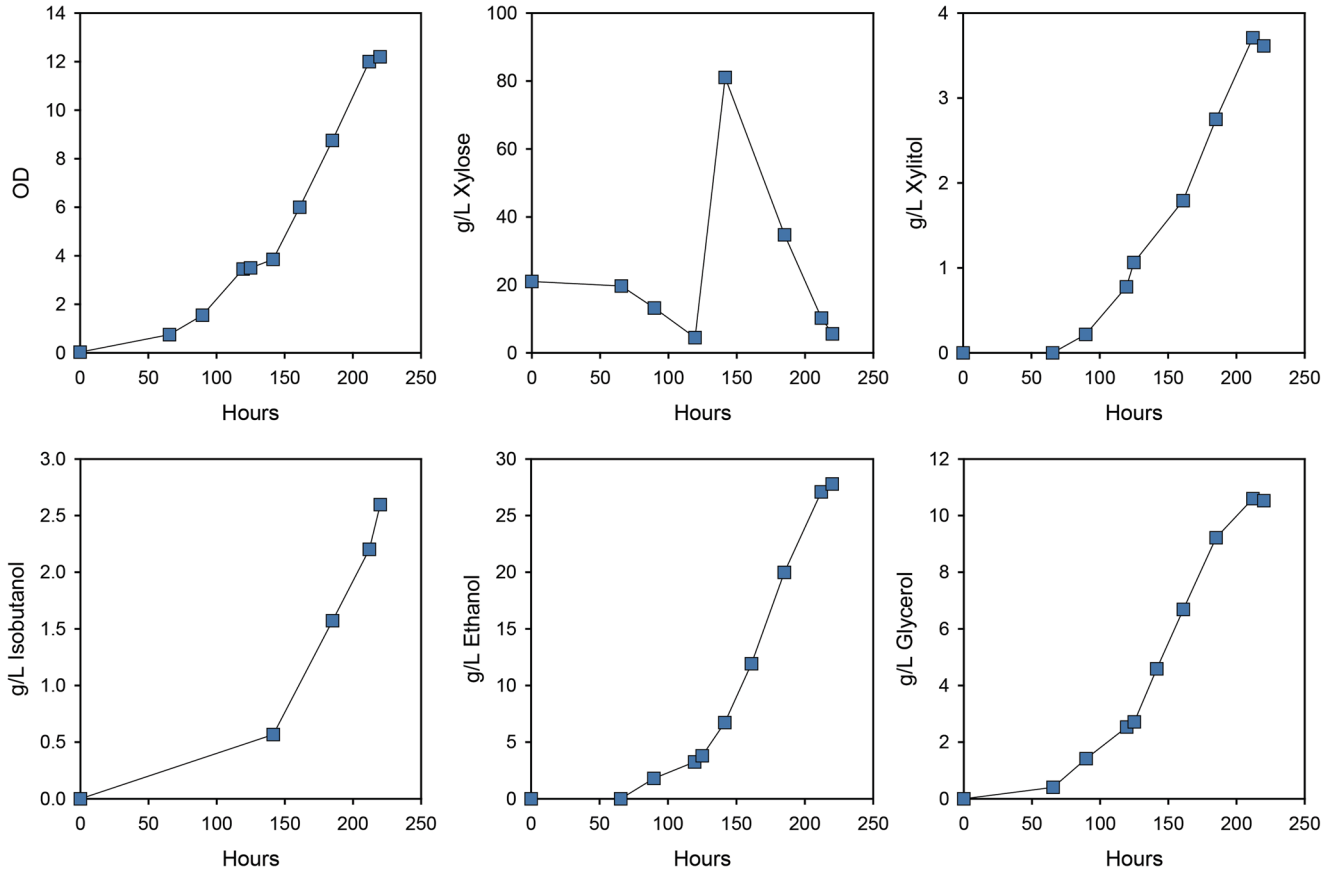

FIGURE 5 Isobutanol production in a 1 L bioreactor. One-liter bioreactor fermentation with SR8-Iso starting with 20 g/L initial xylose followed by a pulse to 80 g/L xylose after 150 hr of fermentation. The fermentation was inoculated with a cell density equal to an OD_{600} of 0.03 in the NRV medium. Agitation was set to 200 rpm, the gas flow was set to 0.5, and pH was maintained at 5.8 using 5 M NaOH. NRV, nutrient-rich Verduyn; OD, optical density; rpm, rotations per minute [Color figure can be viewed at wileyonlinelibrary.com]

4 | DISCUSSION

Although there have been prior reports of production of isobutanol from xylose using engineered *S. cerevisiae*, the initial report produced only 1.36 ± 0.11 mg/L isobutanol from the consumption of 12 g/L of xylose (Brat & Boles, 2013). Compared with strain SR8-Iso developed in this study, the first report used engineered yeast strains with slower xylose consumption rates. While we observe that xylose consumption rates benefit isobutanol production in SR8-Iso, it is possible that consumption rates can become too slow for optimal production of isobutanol from xylose. A more recent publication reports up to 110 mg/L of isobutanol produced from xylose with consumption rates similar to those reported here (Generoso, Brinek, Dietz, Oreb, & Boles, 2017). However, the isobutanol production pathways in both of these previous reports were localized to the cytosol instead of the mitochondria, which may not take full advantage of the respiratory response that xylose induces in yeast engineered to utilize this sugar (Jin, Laplaza, & Jeffries, 2004). Our over 23-fold improvement in production titer shows that the utilization of xylose to produce isobutanol is a problem worth revisiting. We report here a maximum titer of 2.56 ± 0.06 g/L isobutanol using a fed-batch flask fermentation and 2.6 g/L of isobutanol in a bioreactor. In a separate companion publication, a yeast strain engineered with a mitochondrial isobutanol production pathway that instead consumes xylose via the isomerase pathway produces as much as 3.10 ± 0.18 g/L isobutanol, as well as 0.91 ± 0.02 g/L of 2-methyl-1-butanol (Y. Zhang et. al., 2019)

Xylose assimilation redirects carbon flux from ethanol to isobutanol in SR8-Iso, a trend that would likely be amplified if ethanol biosynthesis was genetically disrupted. Deletion of the *PDC1*, *PDC5*, or *PDC6* encoding pyruvate decarboxylase (PDC) isoforms has been used to enhance production of nonethanol compounds, such as lactic acid, (2R,3R)-butanediol, and isobutanol (Baek et al., 2017; Kondo et al., 2012; Lian, Chao, & Zhao, 2014). While deleting one or two of these genes can result in some improvement in yields of the desired product, by lowering ethanol production without dramatically reducing fermentation efficiency, all three genes must be deleted to eliminate ethanol production entirely. However, the simultaneous deletion of *PDC1*, *PDC5*, and *PDC6* substantially decrease strain fitness, complicating isobutanol production (Milne, Wahl, van Maris, Pronk, & Daran, 2016). A more effective strategy to draw metabolic flux from ethanol to isobutanol has been used to dynamically control the expression of *PDC1* and *ILV2* in a

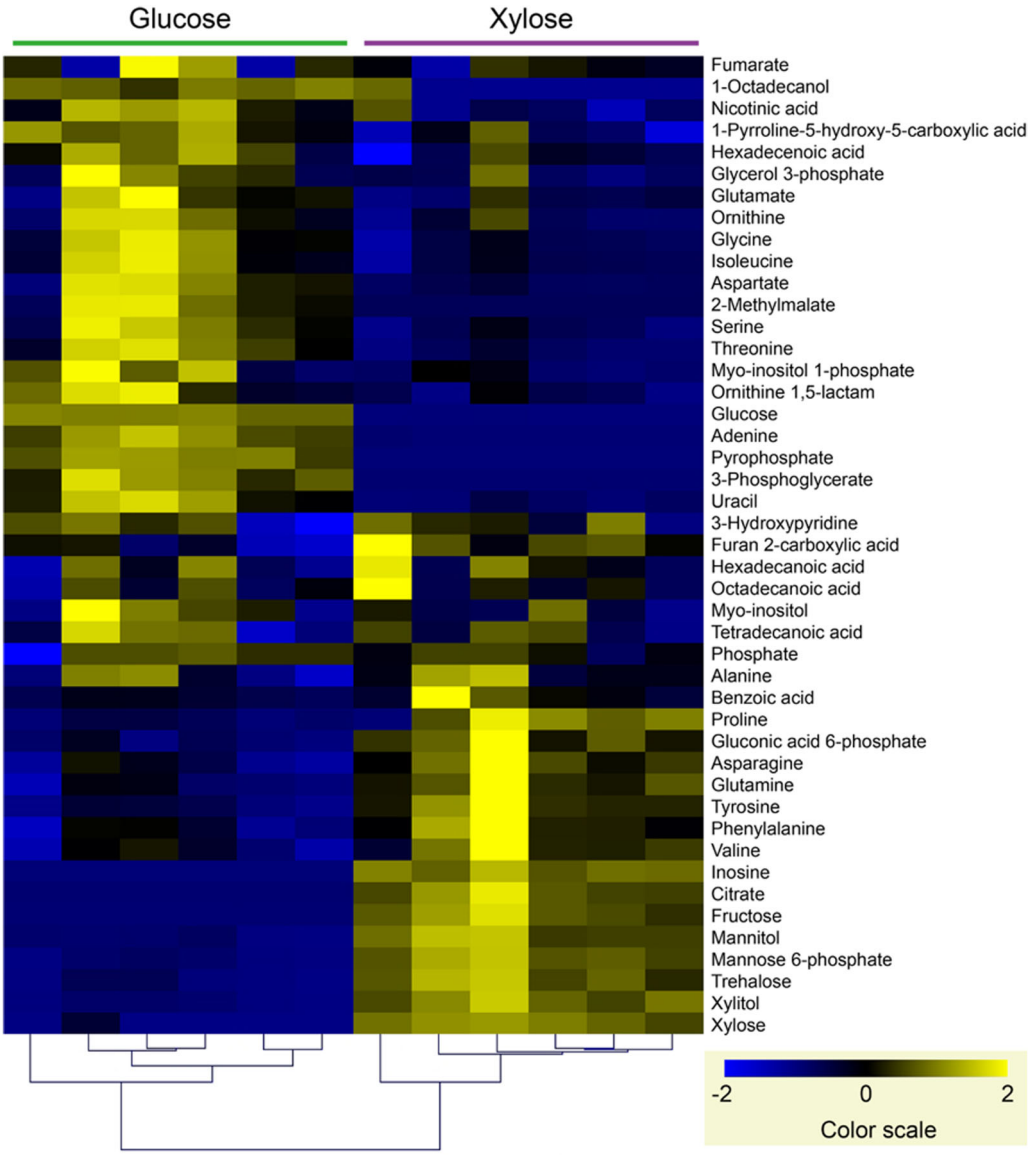

FIGURE 6 Carbon source affects the metabolite profile of the SR8-Iso strain. Metabolite profiles of the SR8-Iso strain cultured on either glucose or xylose. Metabolites were extracted and quantified from cells grown in the mid-exponential phase as described in the materials and methods. Each column represents one biological replicate while each row represents a single metabolite [Color figure can be viewed at wileyonlinelibrary.com]

triple-*PDC* deletion strain background (Zhao et al., 2018), which would likely help to further improve isobutanol production from xylose in SR8-Iso.

When grown in a bioreactor with xylose, SR8-Iso accumulates glycerol and xylitol to as much as 11 g/L and 4 g/L, respectively (Figure 5). A flask fermentation with 80 g/L initial xylose also leads to an accumulation of around 8 g/L glycerol with 2 g/L xylitol (Figure S4). In *S. cerevisiae*, glycerol plays a key role in redox balancing by generating additional NAD^+ (Brisson, Vohl, St-Pierre, Hudson, & Gaudet, 2001). On the other hand, the conversion of xylitol to xylulose consumes NAD^+. The simultaneous accumulation of both metabolites strongly indicates a suboptimal redox balance. Thus, isobutanol production from xylose might be further enhanced by improving redox balance, such as by expressing the NADH oxidase encoded by the *L. lactis noxE* gene (S. J. Kim et al., 2017).

Our metabolite profiling data identified carbon source-dependent differences in cellular valine concentrations. Valine is produced in yeast from α-ketoisovalerate by the branched-chain amino acid transaminases (BCATs) encoded by *BAT1* and *BAT2*. We found that SR8-Iso accumulates more valine when grown in xylose than in glucose, consistent with xylose enhancement of flux through isobutanol biosynthesis, which includes α-ketoisovalerate as a precursor (Figure 1). We have previously shown that deleting *BAT1*, which encodes for the mitochondrial BCAT, enhances mitochondrial isobutanol production (Hammer & Avalos, 2017). Therefore, given the observed accumulation of valine in SR8-Iso, we expect that deleting *BAT1* from this strain will further enhance isobutanol production from xylose.

The slower consumption of xylose as compared with glucose might also play a role in increasing isobutanol production.

Recently, it has been shown that implementing a flux valve increases the yield of isobutanol from engineered *S. cerevisiae* (Tan, Manchester, & Prather, 2016). Endogenous hexokinases *GLK1* and *HXK2* were deleted alongside downregulation of *HXK1* using a doxycycline-inducible repressor, leading to a reduced rate of glucose phosphorylation and lowered glycolytic flux. The addition of the same isobutanol production vector used in this study, pJA180, led to a nearly threefold improvement in production yields. In a future study, it may be interesting to see how the xylose consumption rate influences the yield of isobutanol by using a set of strains with varied xylose consumption capabilities. Such a set of strains has been created in the past by varying the expression level of transaldolase *TAL1* (Xu et al., 2016), a key player in the pentose phosphate pathway and a major determinant of the overall xylose consumption rate.

Glucose induces the Crabtree effect in *S. cerevisiae* (Diaz-Ruiz, Rigoulet, & Devin, 2011) and is known to repress mitochondria biogenesis compared with nonfermentative carbon sources such as glycerol (Egner et al., 2002). In contrast, xylose is not recognized as a fermentable carbon source and induces a respiratory response in yeast engineered to consume it (Belinchón & Gancedo, 2003; Brink, Borgström, Tueros, & Gorwa-Grauslund, 2016; Jin et al., 2004; Osiro, Borgström, Brink, Fjölnisdóttir, & Gorwa-Grauslund, 2019; Osiro et al., 2018). Considering that the isobutanol production pathway in SR8-Iso is compartmentalized in the mitochondria, it is likely that increased mitochondrial biogenesis is a major contributor to the enhanced isobutanol yields from xylose we observe. However, other physiological changes induced by xylose that could divert flux from ethanol to isobutanol production may still be taking place, which would be consistent with several examples where engineered biosynthetic pathways are enhanced by xylose utilization without involving their compartmentalization in mitochondria (S. K. Kim, Jo, Park, Jin, & Seo, 2017; Koivistoinen et al., 2013; Kwak, Kim et al., 2017; Salusjärvi et al., 2017; Turner et al., 2015). Future research to elucidate what physiological changes brought by xylose are responsible for this product biosynthesis enhancement may provide new insights to engineer strains with improved bioconversion of glucose into isobutanol and other nonethanol products.

Although the price of xylose is currently high while availability remains low, full incorporation of lignocellulosic biomass into the biorenewable economy will make xylose an inexpensive and abundant sugar. As reported in this and prior studies, xylose can be an effective substrate for the production of nonethanol products due to the unique physiology and gene regulation present during xylose metabolism by engineered yeast. Furthermore, the economic viability of lignocellulosic biofuels and other bioproducts will depend on utilizing the hemicellulosic fraction of this biomass. Therefore, a future direction of this study is to develop strains that can co-utilize glucose and xylose for isobutanol production, ideally preserving the physiological advantages provided by xylose.

ACKNOWLEDGMENTS

This study was funded by the DOE Center for Advanced Bioenergy and Bioproducts Innovation, including the U.S. Department of Energy, Office of Science, Office of Biological and Environmental Research Award Numbers DE-SC0018420 (to Y.-S. J.) and DE-SC0019363 (to J. L. A.). Any opinions, findings, and conclusions or recommendations expressed in this publication are those of the author(s) and do not necessarily reflect the views of the U.S. Department of Energy.

ORCID

Stephan Lane http://orcid.org/0000-0001-8041-1579
Yong-Su Jin http://orcid.org/0000-0002-4464-9536
José L. Avalos http://orcid.org/0000-0002-7209-4208

REFERENCES

Avalos, J. L., Fink, G. R., & Stephanopoulos, G. (2013). Compartmentalization of metabolic pathways in yeast mitochondria improves the production of branched-chain alcohols. *Nature Biotechnology*, *31*(4), 335–341. https://doi.org/10.1038/nbt.2509

Baek, S. H., Kwon, E. Y., Bae, S. J., Cho, B. R., Kim, S. Y., & Hahn, J. S. (2017). Improvement of D-lactic acid production in *Saccharomyces cerevisiae* under acidic conditions by evolutionary and rational metabolic engineering. *Biotechnology Journal*, *12*, 1700015. https://doi.org/10.1002/biot.201700015

Bastian, S., Liu, X., Meyerowitz, J. T., Snow, C. D., Chen, M. M. Y., & Arnold, F. H. (2011). Engineered ketol-acid reductoisomerase and alcohol dehydrogenase enable anaerobic 2-methylpropan-1-ol production at theoretical yield in *Escherichia coli*. *Metabolic Engineering*, *13*, 345–352. https://doi.org/10.1016/j.ymben.2011.02.004

Belinchón, M. M., & Gancedo, J. M. (2003). Xylose and some non-sugar carbon sources cause catabolite repression in *Saccharomyces cerevisiae*. *Archives of Microbiology*, *180*, 293–297. https://doi.org/10.1007/s00203-003-0593-9

Bilal, M., Iqbal, H. M. N., Hu, H., Wang, W., & Zhang, X. (2018). Metabolic engineering and enzyme-mediated processing: A biotechnological venture towards biofuel production – A review. *Renewable and Sustainable Energy Reviews*, *82*, 436–447. https://doi.org/10.1016/j.rser.2017.09.070

Bordonal, R. O., Carvalho, J. L. N., Lal, R., de Figueiredo, E. B., de Oliveira, B. G., & La Scala, N. (2018). Sustainability of sugarcane production in Brazil. A review. *Agronomy for Sustainable Development*, *38*, 1–23. https://doi.org/10.1007/s13593-018-0490-x

Brat, D., & Boles, E. (2013). Isobutanol production from D-xylose by recombinant *Saccharomyces cerevisiae*. *FEMS Yeast Research*, *13*(2), 241–244. https://doi.org/10.1111/1567-1364.12028

Brink, D. P., Borgström, C., Tueros, F. G., & Gorwa-Grauslund, M. F. (2016). Real-time monitoring of the sugar sensing in *Saccharomyces cerevisiae* indicates endogenous mechanisms for xylose signaling. *Microbial Cell Factories*, *15*, 1–17. https://doi.org/10.1186/s12934-016-0580-x

Brisson, D., Vohl, M. C., St-Pierre, J., Hudson, T. J., & Gaudet, D. (2001). Glycerol: A neglected variable in metabolic processes? *BioEssays*, *23*, 534–542. https://doi.org/10.1002/bies.1073

Christianson, T. W., Sikorski, R. S., Dante, M., Shero, J. H., & Hieter, P. (1992). Multifunctional yeast high-copy-number shuttle vectors. *Gene*, *110*(1), 119–122. https://doi.org/10.1016/0378-1119(92)90454-W

Diaz-Ruiz, R., Rigoulet, M., & Devin, A. (2011). The Warburg and Crabtree effects: On the origin of cancer cell energy metabolism and of yeast

glucose repression. *Biochimica et Biophysica Acta - Bioenergetics*, *1807*, 568–576. https://doi.org/10.1016/j.bbabio.2010.08.010

Egner, A., Jakobs, S., & Hell, S. W. (2002). Fast 100-nm resolution three-dimensional microscope reveals structural plasticity of mitochondria in live yeast. *Proceedings of the National Academy of Sciences*, *99*, 3370–3375. https://doi.org/10.1073/pnas.052545099

Filip, O., Janda, K., Kristoufek, L., & Zilbermam, D. (2017). Food versus fuel: An updated and expanded evidence. *Energy Economics*, https://doi.org/10.1016/j.eneco.2017.10.033

Generoso, W. C., Brinek, M., Dietz, H., Oreb, M., & Boles, E. (2017). Secretion of 2,3-dihydroxyisovalerate as a limiting factor for isobutanol production in *Saccharomyces cerevisiae*. *FEMS Yeast Research*, *17*, 1–10. https://doi.org/10.1093/femsyr/fox029

Hammer, S. K., & Avalos, J. L. (2017). Uncovering the role of branched-chain amino acid transaminases in *Saccharomyces cerevisiae* isobutanol biosynthesis. *Metabolic Engineering*, *44*, 302–312. https://doi.org/10.1016/j.ymben.2017.10.001

Ho, D. P., Ngo, H. H., & Guo, W. (2014). A mini review on renewable sources for biofuel. *Bioresource Technology*, *169*, 742–749. https://doi.org/10.1016/j.biortech.2014.07.022

van Hoek, P., De Hulster, E., Van Dijken, J. P., & Pronk, J. T. (2000). Fermentative capacity in high-cell-density fed-batch cultures of baker's yeast. *Biotechnology and Bioengineering*, *68*(5), 517–523. https://doi.org/10.1002/(SICI)1097-0290(20000605)68:5<517::AID-BIT5>3.0.CO;2-O

Jin, Y., Laplaza, J. M., & Jeffries, T. W. (2004). *Saccharomyces cerevisiae* engineered for xylose metabolism exhibits a respiratory response. *Applied and Environmental Microbiology*, *70*(11), 6816–6825. https://doi.org/10.1128/AEM.70.11.6816

Kildegaard, K. R., Wang, Z., Chen, Y., Nielsen, J., & Borodina, I. (2015). Production of 3-hydroxypropionic acid from glucose and xylose by metabolically engineered *Saccharomyces cerevisiae*. *Metabolic Engineering Communications*, *2*, 132–136. https://doi.org/10.1016/j.meteno.2015.10.001

Kim, S. K., Jo, J. H., Park, Y. C., Jin, Y. S., & Seo, J. H. (2017). Metabolic engineering of *Saccharomyces cerevisiae* for production of spermidine under optimal culture conditions. *Enzyme and Microbial Technology*, *101*, 30–35. https://doi.org/10.1016/j.enzmictec.2017.03.008

Kim, S., Lee, D. Y., Wohlgemuth, G., Park, H. S., Fiehn, O., & Kim, K. H. (2013). Evaluation and optimization of metabolome sample preparation methods for *Saccharomyces cerevisiae*. *Analytical Chemistry*, *85*(4), 2169–2176. https://doi.org/10.1021/ac302881e

Kim, S. R., Park, Y. C., Jin, Y. S., & Seo, J. H. (2013). Strain engineering of *Saccharomyces cerevisiae* for enhanced xylose metabolism. *Biotechnology Advances*, *31*, 851–861. https://doi.org/10.1016/j.biotechadv.2013.03.004

Kim, S. J., Sim, H. J., Kim, J. W., Lee, Y. G., Park, Y. C., & Seo, J. H. (2017). Enhanced production of 2,3-butanediol from xylose by combinatorial engineering of xylose metabolic pathway and cofactor regeneration in pyruvate decarboxylase-deficient *Saccharomyces cerevisiae*. *Bioresource Technology*, *245*, 1551–1557. https://doi.org/10.1016/j.biortech.2017.06.034

Kim, S. R., Skerker, J. M., Kang, W., Lesmana, A., Wei, N., Arkin, A. P., & Jin, Y. S. (2013). Rational and evolutionary engineering approaches uncover a small set of genetic changes efficient for rapid xylose fermentation in *Saccharomyces cerevisiae*. *PLOS One*, *8*(2), e57048. https://doi.org/10.1371/journal.pone.0057048

Koivistoinen, O. M., Kuivanen, J., Barth, D., Turkia, H., Pitkänen, J. P., Penttilä, M., & Richard, P. (2013). Glycolic acid production in the engineered yeasts *Saccharomyces cerevisiae* and *Kluyveromyces lactis*. *Microbial Cell Factories*, *12*(1), 1–16. https://doi.org/10.1186/1475-2859-12-82

Kondo, T., Tezuka, H., Ishii, J., Matsuda, F., Ogino, C., & Kondo, A. (2012). Genetic engineering to enhance the Ehrlich pathway and alter carbon flux for increased isobutanol production from glucose by *Saccharomyces cerevisiae*. *Journal of Biotechnology*, *159*, 32–37. https://doi.org/10.1016/j.jbiotec.2012.01.022

Kopka, J., Schauer, N., Krueger, S., Birkemeyer, C., Usadel, B., Bergmüller, E., & Steinhauser, D. (2005). GMD@CSB.DB: The Golm metabolome database. *Bioinformatics*, *21*, 1635–1638. https://doi.org/10.1093/bioinformatics/bti236

Kwak, S., & Jin, Y.-S. S. (2017). Production of fuels and chemicals from xylose by engineered *Saccharomyces cerevisiae*: A review and perspective. *Microbial Cell Factories*, *16*, 82.

Kwak, S., Kim, S. R. S. R., Xu, H., Zhang, G. C. G.-C., Lane, S., Kim, H., & Jin, Y. S. Y.-S. (2017). Enhanced isoprenoid production from xylose by engineered *Saccharomyces cerevisiae*. *Biotechnology and Bioengineering*, *114*(11), 2581–2591. https://doi.org/10.1002/bit.26369

Lane, S., Dong, J., & Jin, Y.-S. (2018). Value-added biotransformation of cellulosic sugars by engineered *Saccharomyces cerevisiae*. *Bioresource Technology*, *260*, 380–394. https://doi.org/10.1016/j.biortech.2018.04.013

Lian, J., Chao, R., & Zhao, H. (2014). Metabolic engineering of a *Saccharomyces cerevisiae* strain capable of simultaneously utilizing glucose and galactose to produce enantiopure (2R,3R)-butanediol. *Metabolic Engineering*, *23*, 92–99. https://doi.org/10.1016/j.ymben.2014.02.003

Marques, S., Moreno, A. D., Ballesteros, M., & Gírio, F. (2017). Starch biomass for biofuels, biomaterials, and chemicals. In Vaz, S. (Ed.), *Biomass and green chemistry: Building a renewable pathway*. Cham, Switzerland: Springer.

Milne, N., Wahl, S. A., van Maris, A. J. A., Pronk, J. T., & Daran, J. M. (2016). Excessive by-product formation: A key contributor to low isobutanol yields of engineered *Saccharomyces cerevisiae* strains. *Metabolic Engineering Communications*, *3*, 39–51. https://doi.org/10.1016/j.meteno.2016.01.002

Moysés, D. N., Reis, V. C. B., de Almeida, J. R. M., de Moraes, L. M. P., & Torres, F. A. G. (2016). Xylose fermentation by *Saccharomyces cerevisiae*: Challenges and prospects. *International Journal of Molecular Sciences*, *17*(3), 207. https://doi.org/10.3390/ijms17030207

Mumberg, D., Müller, R., & Funk, M. (1995). Yeast vectors for the controlled expression of heterologous proteins in different genetic backgrounds. *Gene*, *156*, 119–122. https://doi.org/10.1016/0378-1119(95)00037-7

Ochs, M. F., Casagrande, J. T., & Davuluri, R. V. (2010). Biomedical informatics for cancer research: Introduction. In Ochs, M., Casagrande, J., & Davuluri, R. (Eds.), *Biomedical informatics for cancer research*. Boston, MA: Springer.

Osiro, K. O., Borgström, C., Brink, D. P., Fjölnisdóttir, B. L., & Gorwa-Grauslund, M. F. (2019). Exploring the xylose paradox in *Saccharomyces cerevisiae* through in vivo sugar signalomics of targeted deletants. *Microbial Cell Factories*, *18*, 88. https://doi.org/10.1186/s12934-019-1141-x

Osiro, K. O., Brink, D. P., Borgström, C., Wasserstrom, L., Carlquist, M., & Gorwa-Grauslund, M. F. (2018). Assessing the effect of D-xylose on the sugar signaling pathways of *Saccharomyces cerevisiae* in strains engineered for xylose transport and assimilation. *FEMS Yeast Research*, *18*, 1–15. https://doi.org/10.1093/femsyr/fox096

Salusjärvi, L., Toivari, M., Vehkomäki, M. L., Koivistoinen, O., Mojzita, D., Niemelä, K., … Ruohonen, L. (2017). Production of ethylene glycol or glycolic acid from D-xylose in *Saccharomyces cerevisiae*. *Applied Microbiology and Biotechnology*, *101*(22), 8151–8163. https://doi.org/10.1007/s00253-017-8547-3

Stein, S. E. (1999). An integrated method for spectrum extraction and compound identification from gas chromatography/mass spectrometry data. *Journal of the American Society for Mass Spectrometry*, *10*, 770–781. https://doi.org/10.1016/S1044-0305(99)00047-1

Styczynski, M. P., Moxley, J. F., Tong, L. V., Walther, J. L., Jensen, K. L., & Stephanopoulos, G. N. (2007). Systematic identification of conserved metabolites in GC/MS data for metabolomics and biomarker

discovery. *Analytical Chemistry*, *79*, 966–973. https://doi.org/10.1021/ac0614846

Tan, S. Z., Manchester, S., & Prather, K. L. J. (2016). Controlling central carbon metabolism for improved pathway yields in *Saccharomyces cerevisiae*. *ACS Synthetic Biology*, *5*(2), 116–124. https://doi.org/10.1021/acssynbio.5b00164

Turner, T. L., Zhang, G. C., Kim, S. R., Subramaniam, V., Steffen, D., Skory, C. D., … Jin, Y. S. (2015). Lactic acid production from xylose by engineered *Saccharomyces cerevisiae* without *PDC* or *ADH* deletion. *Applied Microbiology and Biotechnology*, *99*(19), 8023–8033. https://doi.org/10.1007/s00253-015-6701-3

Xu, H., Kim, S., Sorek, H., Lee, Y., Jeong, D., & Kim, J. (2016). PHO13 deletion-induced transcriptional activation prevents sedoheptulose accumulation during xylose metabolism in engineered Saccharomyces cerevisiae. *Metabolic Engineering*, *34*, 88–96.

Yun, E. J., Oh, E. J., Liu, J. J., Yu, S., Kim, D. H., Kwak, S., … Jin, Y. S. (2018). Promiscuous activities of heterologous enzymes lead to unintended metabolic rerouting in *Saccharomyces cerevisiae* engineered to assimilate various sugars from renewable biomass. *Biotechnology for Biofuels*, *11*, 140. https://doi.org/10.1186/s13068-018-1135-7

Zhang, G. C., Kong, I. I., Kim, H., Liu, J. J., Cate, J. H. D., & Jin, Y. S. (2014). Construction of a quadruple auxotrophic mutant of an industrial polyploid *Saccharomyces cerevisiae* strain by using RNA-guided Cas9 nuclease. *Applied and Environmental Microbiology*, *80*(24), 7694–7701. https://doi.org/10.1128/AEM.02310-14

Zhang, Y., Lane, S., Chen, J. M., Hammer, S., Luttinger, J., Yang, L., …Avalos, J. L. (2019). Xylose utilization stimulates mitochondrial production of isobutanol and 2-methyl-1-butanol in *Saccharomyces cerevisiae*. *Biotechnology for Biofuels*, *12*, 1–15. https://doi.org/10.1186/s13068-019-1560-2

Zhao, E. M., Zhang, Y., Mehl, J., Park, H., Lalwani, M. A., Toettcher, J. E., & Avalos, J. L. (2018). Optogenetic regulation of engineered cellular metabolism for microbial chemical production. *Nature*, *555*, 683–687. https://doi.org/10.1038/nature26141

SUPPORTING INFORMATION

Additional supporting information may be found online in the Supporting Information section.

How to cite this article: Lane S, Zhang Y, Yun EJ, et al. Xylose assimilation enhances the production of isobutanol in engineered *Saccharomyces cerevisiae*. *Biotechnology and Bioengineering*. 2020;117:372–381. https://doi.org/10.1002/bit.27202